SciMedCentral

Journal of Pharmacology & Clinical Toxicology

Research Article

The Effect of Pegylated Liposomal Doxorubicin HCl on Cellular Mitochondrial Function

Fathima S. Ameer, Xiaomin Zhang, Gohar Azhar, and Jeanne Y. Wei*

Department of Geriatrics, University of Arkansas for Medical Sciences, USA

***Corresponding author**

Jeanne Y. Wei, UAMS Donald W. Reynolds Institute on Aging, University of Arkansas for Medical Sciences, 4301 W. Markham, # 748, Little Rock, AR 72205, USA, Tel: 501-603-1261; Fax: 501-686-5300; Email: weijeanne@uams.edu

Submitted: 04 January 2018

Accepted: 31 January 2018

Published: 31 January 2018

ISSN: 2333-7079

Keywords

- Nanoparticle drug-delivery
- Lipo-doxo
- C2C12 myoblasts
- Mitochondrial damage

Abstract

Pegylated liposomal doxorubicin HCl (Lipo-doxo) is one of the leading approved nanoparticle chemotherapeutic drugs widely used to treat variety of cancers and has demonstrated the most significant reduction in risk for cardiotoxicity compared to non-liposomal, conventional doxorubicin. Despite the fact that Lipo-doxo may target mitochondria either directly or indirectly, few data are available regarding cellular bioenergetics on the regulation of mitochondrial fission and fusion genes. In this work, C2C12 myoblast cells have been used as an in-vitro model to study cellular bioenergetics, variations in gene expressions, and biochemical alterations induced by Lipo-doxo under high glucose (25 mM) and normal glucose (5.5 mM) conditions. In C2C12 myoblast cells, Lipo-doxo treatment significantly reduced both mitochondrial oxygen consumption rate (OCR) and extracellular acidification rate (ECAR) under both glucose conditions in a dose dependent manner. Furthermore, Lipo-doxo treatment dysregulated the expression of mitochondrial fission and fusion genes. This dysregulation of mitochondrial fission and fusion genes may influence transformation of the network's connectivity. Using confocal microscopy of C2C12 myoblast cells, we showed that treatment of C2C12 cells with 30 µg/mL Lipo-doxo under high glucose and normal glucose conditions, induced cellular defects. This study provided a better characterization of the effect of Lipo-doxo induced cardiotoxicity.

ABBREVIATIONS

Lipo-doxo: Pegylated Liposomal Doxorubicin HCl; PGC-1α: Peroxisome Proliferator-Activated Receptor Gamma Coactivator-1alpha; PGC-1β: Peroxisome Proliferator-Activated Receptor Gamma Coactivator-1beta; DRP: Dynamin-Related Protein 1; FIS1: Fission1; MFN1: Mitofusin1; MFN2: Mitofusin2; OCR: Oxygen Consumption Rate; ECAR: Extracellular Acidification Rate; qRT-PCR: Quantitative Reverse Transcription PCR; DMEM: Dulbecco's Modified Eagle's Medium; FBS: Fetal Bovine Serum; PBS: Phosphate Buffer Saline; NA: Numerical Aperture; cDNA: Complementary DNA; 2-DG: 2-deoxy-D-Glucose; FCCP: Trifluoromethoxy Carbonyl Cyanide Phenylhydrazone; SD: Standard Deviation

INTRODUCTION

Epidemiological evidence suggests that diabetics are at significantly higher risk for different types of cancer [1,2]. The presence of high blood sugars or hyperglycemia during chemotherapy for hematologic and solid tumors has been shown to correlate with increased toxicity for cancer cells as well as normal tissues. Data suggest that better glycemic control during chemotherapy might maintain the toxicity for cancer cells while protecting normal, non-cancerous cells from chemotherapy-induced damage and improving the outcome of cancer patients [3,4].

Doxorubicin is a very commonly used drug for breast cancer treatment and the use of non-liposomal doxorubicin has been associated with significant cardiotoxicity [2,3]. The current use of polyethylene glycol coated (pegylated) liposomal doxorubicin HCl (Lipo-doxo), has a better safety profile and it is one of the leading approved nanoparticle products used in cancer therapy [2,3]. Pegylated liposomes are less extensively taken up by cells of the reticuloendothelial system and have a tendency to "leak" drug while in circulation, resulting in localization of doxorubicin via leaky vasculature in the tumor tissues [5,6]. It is well known that the cardiac muscle has a high concentration of mitochondria and is very vulnerable to damage from oxidative stress [7-9]. In mitochondria, doxorubicin is reduced to a reactive semiquinone by complex I, reoxidizing to the original form by univalent reduction of oxygen [10].

Mitochondrial morphology is very dynamic in nature with mitochondrial fission and fusion processes [11, 12]. A number of proteins regulate these processes including, dynamin-related protein 1 (DRP1) and fission1 (FIS1) for mitochondrial fission and nuclear-encoded mitochondrial proteins, MFN1 and MFN2 for fusion [13-15]. Impairment of the mitochondria by

chemotherapeutic agents such as doxorubicin could severely affect cellular homeostasis and result in cardiac dysfunction with increased morbidity and mortality [16]. In the setting of diabetes or high blood sugars, the toxic effect of chemotherapy could be enhanced. Hence, the optimal nutrient conditions to protect non-cancerous cells from detrimental effects chemotherapy requires further investigation.

The current study has several objectives: 1) to analyze mitochondrial respiration and glycolysis using a flux analyzer in C2C12 cells treated with different concentrations of Lipo-doxo under glucose stress conditions; 2) to evaluate the gene expression in C2C12 myoblast cells treated with Lipo-doxo; 3) to assess alterations in cell morphology in C2C12 cells in response to Lipo-doxo treatment.

MATERIALS AND METHODS

Reagents

Dulbecco's modified Eagle's medium (DMEM), glutamine, penicillin, streptomycin, and fetal bovine serum (FBS) were purchased from Gibco-Invitrogen (Grand Island, NY, USA). Pegylated liposomal doxorubicin (Doxil) was purchased from FormuMax Scientific (Silicon Valley, CA, USA). Mito Tracker Red CMXRos was purchased from ThermoFisher Scientific (Eugene, OR, USA).

Cell culture

The DMEM media containing 10% (v/v) FBS with two different clinically relevant glucose concentrations were used in the present study: normal (100 mg/dL or 5.5 mM) and high (450 mg/dL or 25 mM). Mouse musmusculus myoblast (C2C12) cells were purchased from American Type Culture Collection (Manassas, VA). C2C12 cells were cultured in BD Falcon 75 cm^2 flasks, containing DMEM with 2 mM L-glutamine, supplemented with 10% (v/v) FBS, and penicillin G and streptomycin. Cell cultures were incubated at 37 °C in 5% CO_2. Primary cultures received new medium 24 h after seeding and were sub-cultured upon reaching more than 80% confluence by the use of 0.25% trypsin-EDTA, inactivated by trypsin neutralizing solution (Invitrogen).

Mitochondrial function assay

Mitochondrial function was assayed using an XF96 Extracellular Flux Analyzer (Seahorse Bioscience, North Billerica, MA) following manufacturer's instructions. Briefly, C2C12 myoblast cells were seeded in XF96 cell culture plates (Seahorse Bioscience) in 80 µL of high glucose medium (or normal glucose medium) and cultured to 80% confluence overnight at 37 °C in a humidified incubator with 5% CO_2. Prior to the Lipo-doxo treatment, the growth medium in the well of the XF cell plate was replaced with fresh growth medium. Cells not exposed to Lipo-doxo served as controls in each experiment. When cells reached sub-confluence, they were pre-treated for 24 h with 0, 15, and 30 µg/mL Lipo-doxo. Following treatment, the culture supernatant was removed and cells were washed three times with phosphate-buffered saline (PBS). Prior to the assay, the growth medium in the well of the XF cell plate was replaced with the appropriate assay medium. The sensor cartridge was calibrated, and the cell plate was incubated at 37 °C for one hour. All experiments were performed at 37 °C.

Measurement of oxygen consumption rate (OCR)

Mitochondrial respiration was measured using an XF Cell Mito Stress Test Kit (Seahorse Biosciences Billerica, MA, USA) following the manufacturer's instructions. The following compounds were injected: oligomycin (2 µM), an ATP synthetase inhibitor; FCCP (0.5 µM), an uncoupler reagent; rotenone (0.5 µM), a mitochondrial complex I inhibitor; and antimycin A (0.5 µM), a mitochondrial complex III inhibitor.

Measurement of extra cellular acidification rate (ECAR)

The glycolysis assay was performed using an XF Glycolysis Stress test Kit (Seahorse Biosciences Billerica, MA) following the manufacturer's instructions. Glycolysis, glycolytic capacity, and non-glycolytic acidification were calculated as for ECAR. The following compounds were injected: glucose (10 mM); oligomycin (2 µM), an ATP synthetase inhibitor; 2-deoxy-D-glucose (50 mM), glycolysis inhibitor.

Quantitative reverse transcription PCR (qRT-PCR)

C2C12 cells were cultured in six-well plates to 80% confluence in normal glucose medium, after which the cells were either remained in normal glucose medium, or were subjected to high glucose treatment. After that, the cells were pre-treated for 24 h with 30 µg/mL Lipo-doxo. Following incubation, total cellular RNA was extracted from cells using miRNeasy Mini Kit and RNase-free DNase I digestion (Qiagen, Valencia, CA) in accordance with the manufacture's recommendations for mammalian cells. RNA with a high RNA integrity number and an A260 and A280 absorbance ratio ranging from 1.8 to 2.1 was utilized for cDNA synthesis. To quantitate the expression of the mRNA, real-time qRT-PCR was performed. To select a proper internal loading control for real-time qRT-PCR, we examined the expression of 5S ribosomal RNA (5S RNA) and 18S in Lipo-doxo treated versus untreated C2C12 cells, we found that the expression of 5S RNA remained unchanged in Lipo-doxo treated versus untreated C2C12 cells, while 18S expression changed significantly in Lipo-doxo treated versus untreated C2C12 cells. Therefore, 5S RNA was used as an internal loading control. The PCR amplification was performed in a 7900HT Fast Sequence Detector System (Applied Biosystems). C_T values were automatically obtained. Relative expression values were obtained by normalizing C_T values of the mRNA genes in comparison with C_T values of the 5S gene (which was documented to remain unchanged across all the groups), using the delta-delta C_T method.

Confocal microscopy

Briefly, C2C12 cells were seeded onto six-well plates and grown in normal glucose DMEM medium supplemented with 10% FBS at 37 °C and 5% CO_2 for 24 h. Upon attachment and 80% confluence in normal glucose medium, the cells either remained in normal glucose medium, or were subjected to high glucose treatment. Next, C2C12 cells were treated with 30 µg/mL Lipo-doxo for 24 h. Prior to the Lipo-doxo treatment, the growth medium in the six-well plate was replaced with fresh growth

medium. After treatment, the cells were washed with PBS twice and incubated in 150 nM Mito Tracker Red CMXRos (Invitrogen/Molecular Probes, Eugene, OR) in growth medium at 37°C for 1 h. The cells were then washed and fixed in 3.7% formaldehyde for 10 min at room temperature. The fixative was removed by washing with PBS and fresh PBS was replaced for fixed cell imaging. All images were acquired using a 60X/1.4 NA oil objective at room temperature using a Nikon confocal microscope C2/C2si (Nikon, Inc.). A 1 mW and 561 nm wavelength solid-state helium–neon laser was used as the excitation source for confocal microscopy.

Statistical analysis

Data are given as mean ± SD, with n denoting the number of experiments unless otherwise indicated. The differentially expressed mRNAs with at least 1.5-fold changed were identified using a t-test with a cut off p value of either $p < 0.05$ or $p < 0.01$.

RESULTS

Lipo-doxo repressed the mitochondrial oxygen consumption rate (OCR)

We investigated the mitochondrial oxidative phosphorylation in C2C12 cells treated with different concentrations of Lipo-doxo under high glucose (Figure 1A) and normal glucose (Figure 1C) conditions using the Seahorse XF96 Extracellular Flux Analyzer that measures the oxygen consumption rate (OCR). The seeding density and concentrations of the injection compounds were optimized. The mitochondrial stress test used four drugs that interrogate mitochondrial function. Oligomycin inhibits Complex V of the electron transport chain, and injection of this compound showed how much of the OCR was due to ATP synthesis. Subsequent injection of the uncoupler FCCP, a photonophore, allowed protons to move into the mitochondria matrix independent of the ATP synthase. In order to maintain the membrane potential, protons move back into the intermembrane space by increasing the flow of electrons across the electron transport chain to the maximum speed. Thus, injection of FCCP reveals the maximal respiratory capacity of the cells. The ratio of maximal OCR as compared to basal OCR is known as spare respiratory capacity. Rotenone and antimycin A block Complex I and III, respectively, completely inhibit the electron transport chain, and as such any remaining oxygen consumption after these drugs are introduced, is non-mitochondrial.

Here we observed the expected responses in OCR (Figure 1A and Figure 1C) as the C2C12 cells were treated with each successive compound. Compared with vehicle–treated cells, the Lipo-doxo treated cells exhibited a reduction in maximal respiratory capacity, as evidenced by reduced oxygen consumption under high glucose (Figure 1A) and normal glucose (Figure 1C) conditions. Both 15 μg/mL and 30 μg/mL Lipo-doxo concentrations significantly repressed basal respiration of the

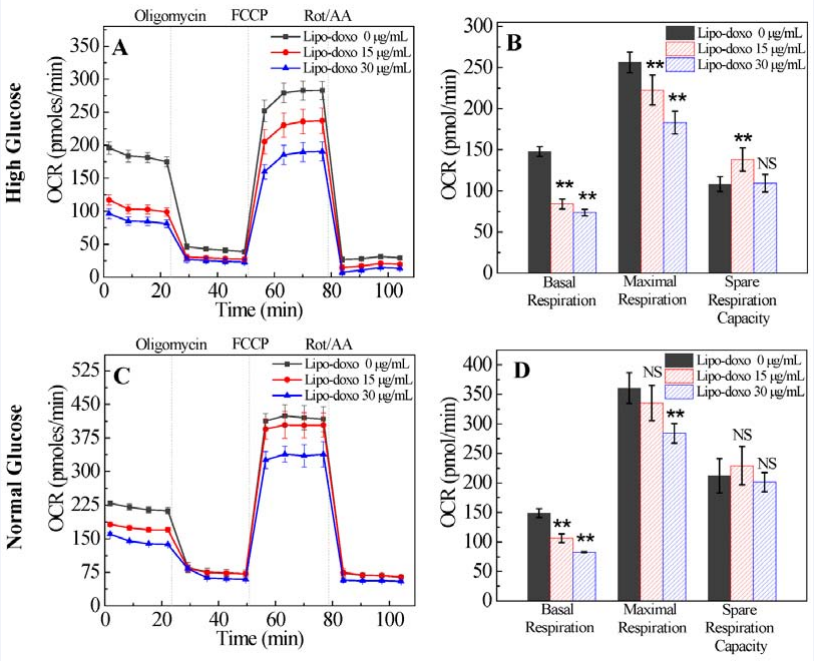

Figure 1 Effect of Lipo-doxo on oxygen consumption rate (OCR) under high glucose (25 mM) vs. normal glucose (5.5 mM) conditions. Lipo-doxo induces metabolic alterations in C2C12 cells. (A) Kinetic OCR responses of Lipo-doxo treated C2C12 cells under high glucose condition. (B) Basal respiration, maximal respiration, and spare respiration capacity were calculated for Lipo-doxo treated and untreated C2C12 cell line under high glucose condition. (C) Kinetic OCR responses of Lipo-doxo treated C2C12 cells under normal glucose condition. (D) Basal respiration, maximal respiration, and spare respiration capacity were calculated for Lipo-doxo treated and untreated C2C12 cell line under normal glucose condition. Asterisks (**) indicate statistically significant differences ($p < 0.01$) between Lipo-doxo untreated and treated C2C12 cells under high and normal glucose conditions. Note that there were clear differences between Lipo-doxo untreated and treated C2C12 cells under high and normal glucose conditions for basal respiration, which was significantly decreased in Lipo-doxo treated C2C12 cell under high glucose conditions. After 24 h of Lipo-doxo incubation, OCR was measured under basal conditions followed by the sequential addition of oligomycin (2 μM), FCCP (0.5 μM), and rotenone/antimycin A (0.5 μM), as indicated.

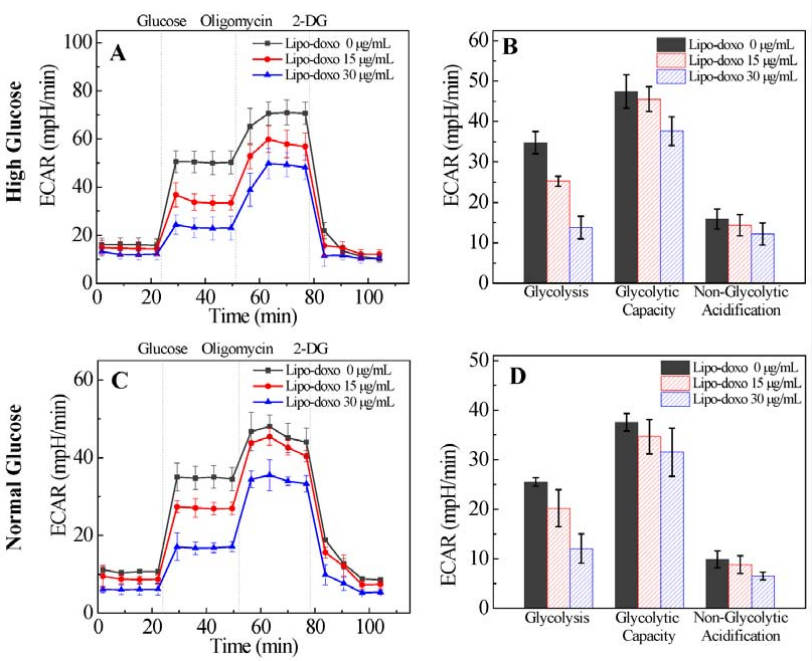

Figure 2 Effect of Lipo-doxo on extracellular acidification rate (ECAR) under high glucose (25 mM) vs. normal glucose (5.5 mM) conditions. (A) Kinetic ECAR responses in Lipo-doxo treated and untreated C2C12 cells under high glucose condition. (B) Glycolysis, glycolytic capacity, and non-glycolytic acidification were calculated for Lipo-doxo treated and untreated C2C12 cells under high glucose condition. (C) Kinetic ECAR responses in Lipo-doxo treated C2C12 cells under normal glucose condition. (D) Glycolysis, glycolytic capacity, and non-glycolytic acidification were calculated for Lipo-doxo treated and untreated C2C12 cells under normal glucose condition. After 24 h of Lipo-doxo incubation, ECAR was measured under basal conditions followed by the sequential addition of 10 mM glucose, 2 μMoligomycin, and 50 mM 2-Deoxy-D-glucose (2-DG). A series of ECAR in C2C12 cells in the presence or absence of Lipo-doxo were examined by Seahorse XF96 analyzer. ECAR following the addition of glucose defines glycolysis and ECAR following oligomycin represents maximum glycolytic capacity. Data are shown as mean ± standard deviation, n = 3.

C2C12 cells at the resting state under high glucose (Figure 1A) and normal glucose (Figure 1C) conditions. When ATPase activity was blocked by oligomycin, ATP production was decreased in both empty vector-treated and Lipo-doxo treated C2C12 cells, which was further decreased in 15 μg/mL and 30 μg/mL Lipo-doxo treated cells. This can be used to distinguish the percentage of oxygen consumption devoted to ATP synthesis and the percentage of oxygen consumption required to overcome the natural proton leak across the inner mitochondrial membrane. Subsequently, FCCP was injected to stimulate maximal capacity of cells for mitochondrial respiration. As shown previously, FCCP acted as an uncoupling agent. Since the cells had to overcome the proton leak across the inner mitochondrial membrane, OCR increased significantly as more O_2 was consumed to pump the excess protons back across the mitochondrial membrane. Finally, rotenone inhibited mitochondrial Complex I and Complex III, respectively, which caused the flow of electrons to cease in the electron transport chain, and thus the consumption of O_2 was drastically reduced. As shown in Figure 1B and Figure 1D data analysis revealed that the different concentrations of Lipo-doxo used in this study repressed basal respiration and maximal respiration under high and normal glucose conditions. Furthermore, the spare respiration capacity was up-regulated for 15 μg/mL Lipo-doxo treated C2C12 cells under high glucose condition. However, there was no significant change in the spare respiration capacity for 30 μg/mL Lipo-doxo treated C2C12 cells under nutrient stress conditions. These results suggested that C2C12 cells under normal glucose condition with or without treatment of Lipo-doxo, possessed higher mitochondrial oxidative phosphorylation activities than C2C12 cells under high glucose condition.

Lipo-doxo altered the glycolytic rate

Previous studies have shown that glycolysis account for ~80% of total ECAR in a number of cancer cells as determined through either removing glucose from the assay medium or adding glycolytic pathway inhibitor such as hexokinase inhibitor 2-DG [17]. The remaining 20% of the ECAR can be attributed to other metabolic processes, such as the tricarboxylic acid cycle CO_2 evolution. The OCR response to glucose, monitored concurrently with ECAR serves as an indicator of whether glucose is also catabolized through mitochondrial respiration (Data not shown).

To determine glycolysis, glycolytic capacity, and non-glycolytic acidification of the C2C12 cells treated with 15 μg/mL and 30 μg/mL Lipo-doxo under high glucose (Figure 2A) and normal glucose (Figure 2C) conditions, we measured ECAR while consecutively injection glucose, oligomycin, and 2-DG. As shown in Figure 2A, glucose addition to C2C12 cells caused an instant increase in kinetic ECAR responses and triggered a glycolytic flux of 35 ± 2.7 mpH/min for control cells, 25 ± 1.2 mpH/min for 15 μg/mL Lipo-doxo treated cells, and 14 ± 2.8 mpH/min for 30 μg/mL Lipo-doxo treated cells under high glucose conditions. The subsequent addition of oligomycin caused a further increase in ECAR to 47 ± 4.1 mpH/min for control cells, 45 ± 3.1 mpH/min

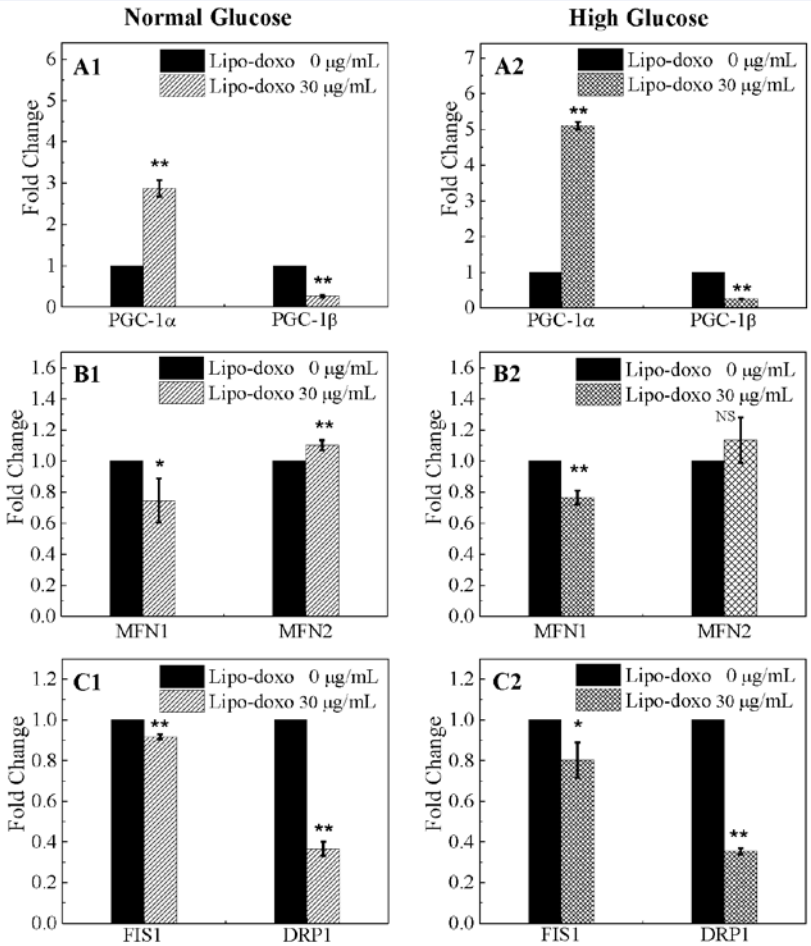

Figure 3 Quantitative reverse transcription PCR (qRT-PCR) validation of changes in the expression of selected genes involved in mitochondrial biogenesis and function. Effect of 30 μg/mL Lipo-doxo for 24 h on (A) PGC-1α and β, (B) MFN1 and 2, and (C) FIS1 and DRP1 genes under high glucose and normal glucose conditions. Cells were harvested for the analysis of gene expression by qRT-PCR, and the data were normalized to those for 5S. * $p < 0.05$ and ** $p < 0.01$. Data are expressed as the mean ± standard deviation of three independent experiments.

for 15 μg/mL Lipo-doxo treated cells, and 37 ± 3.5 mpH/min for 30 μg/mL Lipo-doxo treated cells under high glucose conditions, indicating an elevated glucose flux toward lactate and revealing the glycolysis capacity of C2C12 cells treated with different concentrations of Lipo-doxo. The final addition of glycolysis inhibitor 2-DG abolished the overall glycolysis. Similar results were obtained under normal glucose condition (Figure 2C). The calculated glycolysis, glycolytic capacity, and non-glycolytic acidification for C2C12 cells treated with different concentrations of Lipo-doxo under high and normal glucose conditions are shown in Figure 2B and Figure 2D. Among two different glucose concentration tested in the present study, Lipo-doxo treated and untreated C2C12 cells under high glucose conditions showed higher values for glycolysis, glycolytic capacity, and non-glycolytic acidification (Figure 2B), as compared with the normal glucose conditions (Figure 2D). The concentration of oligomycin and glucose used in this study were optimized to get maximal inhibition of respiration (data not shown).

Dysregulation of mitochondrial fission and fusion genes expression as a result of Lipo-doxo treatment

The effect of Lipo-doxo on the expression of PGC-1α gene and PGC-1β gene, which are upstream regulators of mitochondrial genes, were examined. As shown in Figure 3A1, under high glucose stress condition treatment with C2C12 cells with 30 μg/mL Lipo-doxo for 24 h up-regulated the expression of PGC-1α mRNA level ($p < 0.01$, n = 3), but the expression of PGC-1β mRNA level ($p < 0.01$, n = 3) was down-regulated. Similar effect was observed under normal glucose condition (Figure 3A2).

The PGC-1α is upstream regulator of mitochondrial genes, including mitofusin genes. The MFN1 and MFN2 participate in the regulation of the mitochondrial network [18,19]. As shown in Figure 3B1, we detected the expression levels of MFN1 and MFN2 and observed that MFN1 ($p<0.01$, n= 3) was down-regulated upon 30 μg/mL Lipo-doxo treatment for 24 h under high glucose condition. However, there is no significant change in the expression of MFN2 (NS, n = 3) upon 30 μg/mL Lipo-doxo treatment for 24 h under high glucose condition. As shown in Figure 3B2, under normal glucose condition, when C2C12 cells were treated with 30 μg/mL Lipo-doxo for 24 h MFN1 ($p< 0.05$, n= 3) was down-regulated and MFN2 was up regulated (n = 3$p<$ 0.01).

As shown in Figure 3C1, treatment with 30 μg/mL Lipo-doxo

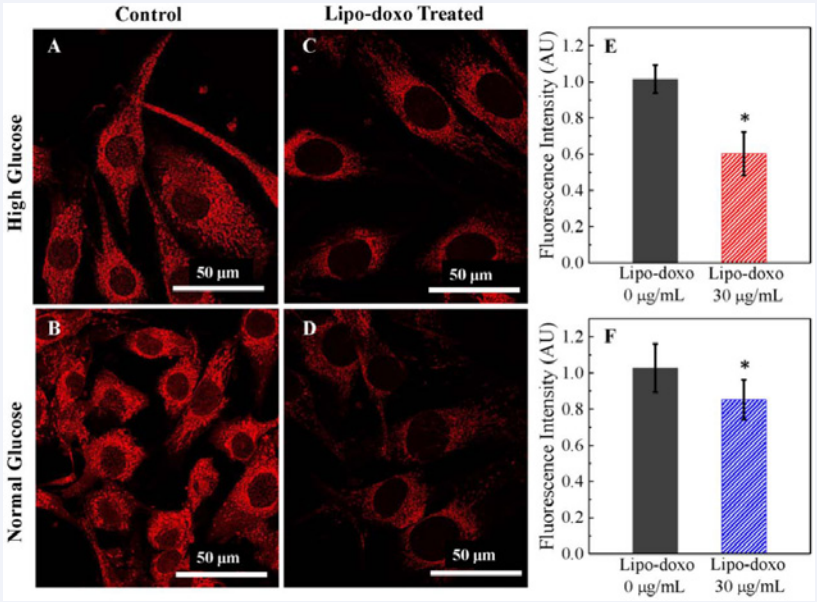

Figure 4 Change in mitochondrial morphology in Lipo-doxo exposed C2C12 cells under different glucose concentrations treatment. Exposure to 30 µg/mL Lipo-doxo under high glucose and normal glucose conditions induces fine structural changes of mitochondria in C2C12 myoblast cells. Cells were stained with Mito tracker red. Confocal microscopy images of C2C12 cells treated with (A, C) 0 µg/mL and (B, D) 30 µg/mL of Lipo-doxo under high glucose (top) and normal glucose (bottom) conditions for 24 h. Quantitation of the intensity of Mito tracker red staining under (E) high glucose and (F) normal glucose conditions. *Denotes statistical difference between a Lipo-doxo treated and the untreated control ($p < 0.05$, n=3). Note that Mito tracker red fluorescence appears to be diminished with Lipo-doxo treatment under high and normal glucose conditions for 24 h. However, mitochondria still maintained some degree of membrane polarization as evidenced by their ability to stain with Mito tracker red. The scale bar of each image is 50 µm. Images were acquired using a 60X oil immersion objective with a NA of 1.40. All images have the same magnification.

for 24 h under high glucose condition repressed the expression of both FIS1 ($p < 0.05$, n = 3) and DRP1 ($p < 0.01$, n = 3) mRNA level. Similar results were observed under normal glucose condition (Figure 3C2) for FIS1 ($p < 0.01$, n = 3) and DRP1 ($p < 0.01$, n = 3) mRNA level.

Lipo-doxo altered the mitochondrial morphology and mitochondrial membrane potential

C2C12 myoblast cells were star-shaped, with a prominent single central nucleus, with numerous nucleoli. By using confocal microscopy, alterations in mitochondrial morphology were evaluated using Mito tracker red (Figure 4). Figure 4A and 4B shows control C2C12 myoblasts with intact cell membranes and filamentous polarized mitochondria under high glucose and normal glucose conditions, respectively. Treatment with 30 µg/mL Lipo-doxo caused breakage of the mitochondrial network under both glucose concentrations (Figure 4C and 4D). Furthermore, loss of the mitochondrial Mito tracker red signal could be seen due to the mitochondrial depolarization induced by Lipo-doxo (Figure 4C and 4D). However, for 30 µg/mL Lipo-doxo concentration tested, the mitochondrial network still accumulated Mito tracker red, demonstrated the retention of a transmembrane electric potential (Figure 4C and 4D).

Perturbation of mitochondrial membrane potential might be associated with various physiological and pathophysiologic processes inside cells, and its determination is widely used for the characterization of cellular and mitochondrial metabolism and viability, as well as apoptosis. Mito tracker red is a mitochondrion selective dye that accumulates in mitochondria in a membrane potential dependent manner. When used in appropriately designed experiments, Mito tracker red has been validated as a noncytotoxic and sensitive indicator of relative changes in mitochondrial membrane potential in several cultured cell types. The effect of 30 µg/mL Lipo-doxo for 24 h on mitochondrial membrane potential was evaluated in C2C12 cells under high glucose and normal glucose conditions. Cells were exposed to 30 µg/mL Lipo-doxo for 24 h and assayed for Mito tracker red uptake using confocal microscope. Mitochondrial staining was punctate in untreated cells (Figure 4A and 4B), indicative of selective uptake and concentration of Mito tracker red by healthy, actively respiring mitochondria. Once taken up by mitochondria, a mildly thiol-reactive chloromethyl moiety is responsible for keeping the dye associated with the organelle [20]. The brightness of the fluorescent intensity was reduced in cells exposed to Lipo-doxo (Figure 4C and 4D) indicates a significant reduction of mitochondrial membrane potential in C2C12 cells (Figure 4E and 4F). Furthermore, some of the cells but not all treated with 30 µg/mL Lipo-doxo for 24 h, exhibited more diffuse Mito tracker red staining throughout the cytosol, a pattern indicative of mitochondrial membrane depolarization (data not shown). This diffuse staining pattern was the result of a lack of healthy mitochondria and thereby reduced uptake of the probe, resulting in diffusion of Mito tracker red throughout the cytoplasm [21].

Treatment with 30 µg/mL Lipo-doxo under high glucose (Figure 5B) and normal glucose (Figure 5D) conditions for 24 h led to alterations in cellular morphology and the cytoplasm appeared to be vacuolated. Nuclear alterations induced by Lipo-

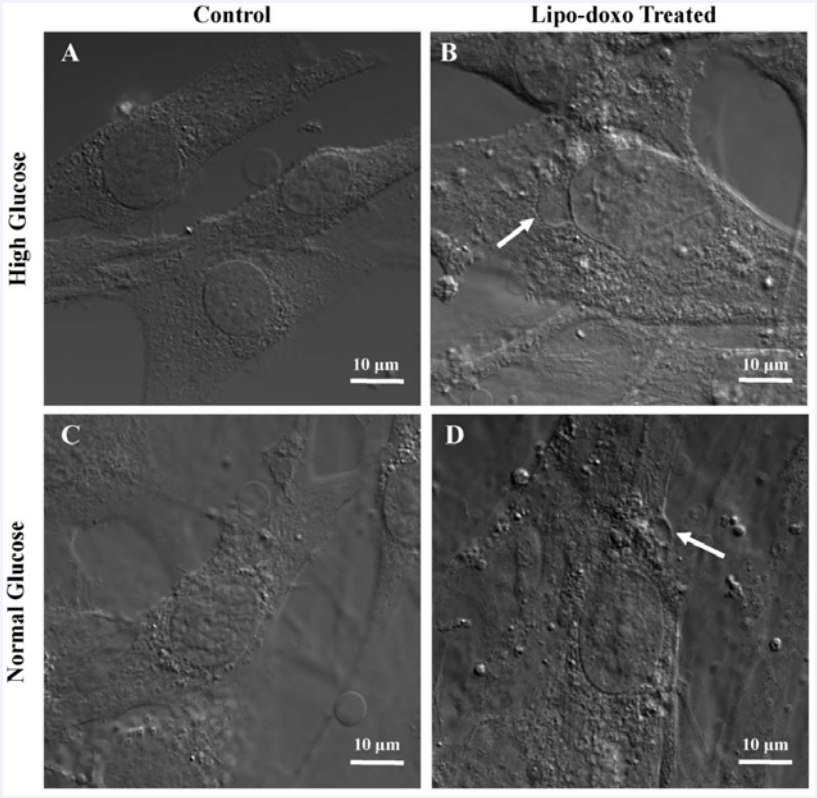

Figure 5 Lipo-doxo induces cytoplasm vacuolization under different glucose conditions. DIC images of C2C12 cells treated with (A, C) 0 µg/mL and (B, D) 30 µg/mL of Lipo-doxo under high glucose (top) and normal glucose (bottom) conditions for 24 h. The scale bar of each image is 10 µm. All images have the same magnification. Arrows indicate Lipo-doxo induced cytoplasmic vacuolization under different glucose conditions.

doxo exposure were also explored in the present work. 30 µg/mL Lipo-doxo cause an increase in the area of cell nuclei under high glucose and normal glucose conditions. The increase in nuclear area was clearly observed by microscopy (Figure 5B and 5D) and was accompanied by what appeared to be nucleoli disorganization. An increase in nuclear size was observed regardless of the degree of vacuolization exhibited by C2C12 cells.

DISCUSSION

The present study has several major findings. In C2C12 myoblast cells, treatment with Lipo-doxo repressed mitochondrial oxygen consumption rate and extracellular acidification rate under high glucose and normal glucose conditions. The presence of Lipo-doxo induced mitochondrial morphological alterations in C2C12 cells and reduced mitochondrial membrane potential. Lipo-doxo treatment down-regulated the expression of MFN1, PGC-1β, FIS1 and DRP1 genes, but up-regulated the expression of MFN2 and PGC-1α genes (Table 1).

In the recent years, targeting mitochondria emerged as an attractive strategy to control mitochondrial dysfunction related diseases. Despite the desire to direct therapeutics to the mitochondria, the actual task is more difficult due to the highly complex nature of the mitochondria. Only a handful of nanoparticles based on metal oxides, gold nanoparticles, dendrons, carbon nanotubes, and liposomes were recently engineered to target mitochondria. Most of these materials face tremendous challenges when administered *in vivo* due to their limited biocompatibility. Among the numerous types of nanocarriers, liposomes emerged as promising delivery systems [22-27].

Our results suggest that the reduced OCR after Lipo-doxo treatment may be due to Complex I damage, and could explain the decline in OCR of C2C12 cells treated with Lipo-doxo for 24 h. Previous reports have shown mitochondrial dysfunction [28], and inactivation of mitochondrial systems such as complexes I, III, IV, and V, and also phosphate carrier [29], and ATP-ADP translocase, partly due to binding of doxorubicin to cardiolipin of the inner mitochondrial membrane [30]. The spare respiratory capacity of mitochondria in response to oxidative stress and energetic insufficiency is important [31,32]. The maximal respiration mainly depends on the function of the substrate supplementation [33]. Souid and coworkers reported that oxidative phosphorylation is enhanced in Jurkat and HL-60 cells exposed to 1 µM non-liposomal conventional doxorubicin for 30 min [34]. They also demonstrated that incubation of cells with high concentrations of non-liposomal conventional doxorubicin (5-20 µM) for 1 h caused a significant inhibition of mitochondrial respiration [35]. Interestingly, C2C12 cells treated with Lipo-doxo under different glucose concentrations significantly changed the sensitivity of mitochondria to the mitochondrial uncoupler FCCP. The sensitivity to FCCP may depend on the conformational state of the mitochondrial inner membrane, such as changes in its fluidity and regularity. We also observed a significant decrease

in ATP levels in Lipo-doxo treated C2C12 cells (data not shown), which points to the major role of mitochondrial oxidative phosphorylation in maintaining energy status. We also assessed the differences in glycolysis-induced ECAR among the Lipo-doxo treated and untreated C2C12 cells under high glucose and normal glucose conditions (Figure 2). The results of the extracellular flux study showed a significant decrease in extracellular acidification rates in glycolysis, glycolytic capacity, and non-glycolytic acidification (Figure 2B and 2D) under normal glucose and high glucose conditions.

Interestingly, we noted that treatment of C2C12 myoblast cells with 30 μg/mL Lipo-doxo for 24 h up-regulated the expression of MFN2. In agreement with this finding, other studies tend to support the idea that increased MFN2 in cardiomyocytes predicts an adverse outcome, promoting cell death through apoptotic or autophagic mechanisms [9]. PGC-1α and PGC-1β are important positive regulators of mitochondrial activity and biogenesis in skeletal muscle [36]. Key mitochondrial processes, such as organelle biogenesis and uncoupling, are differentially regulated by these homologues. It has been shown that PGC-1α stimulates MFN2 gene promoter activity, and increases the expression of MFN2 mRNA and protein expression in both skeletal muscle and brown adipose tissue in conditions associated with enhanced energy expenditure [37]. It is likely that the up-regulation of PGC-1α gene by Lipo-doxo treatment may have affected the expression of MFN2 gene expression. Cells lacking DRP1 contain highly interconnected mitochondrial nets that are formed by ongoing fusion in the absence of fission activity [11]. Previous work using animal models have demonstrated that MFN1 and MFN2 are essential to mitochondrial remodelling during postnatal cardiac development [38]. Mutations in the mitochondrial fission and fusion genes are associated with several human diseases [39].

The mitochondrial membrane potential is a useful tool to monitor changes in the cell's capacity to generate ATP by oxidative phosphorylation [40]. According to the literature, repression of MFN2 caused changes in mitochondrial morphology, reduced the mitochondrial membrane potential, cellular respiration, glucose oxidation and proton leak as well as oxidation of pyruvate and fatty acids [41]. Wallace et al., reported that non-liposomal conventional doxorubicin altered the organization of H9C2 myoblast cardiac sarcomericmyocin [42]. A relation between non-liposomal conventional doxorubicin treatment and alterations in myocardial structural proteins and regulatory protein expression after *in vivo* treatment of rats has also been reported [43].

We also observed an increase in nuclear area after Lipo-doxo treatment under high glucose and normal glucose conditions. Similar nuclear swelling has been described after etoposide treatment of neuronal cells [44]. Changes in nuclear morphology, including chromatin de-condensation, were also observed by electron microscopy [42]. The vacuoles observed in the present study could have originated from sarcoplasmic reticular enlargement [45] or autophagic cell death [46]. Such vacuoles are known to contain products of lipid metabolism or peroxidation [47].

Epidemiological studies have revealed that diabetes is correlated with increased cancer risk [1,2], and that diabetics treated with metformin have reduced risk of developing various types of cancer [48,49]. Metformin is an extensively used and

Table 1: Summary of differences between C2C12 myoblast cells treated with 30 μg/mL Lipo-doxo, under normal glucose and high glucose conditions.

	Normal Glucose (5 mM)	**High Glucose (25 mM)**
	Lipo-doxo treated Mean (±SD)	**Lipo-doxo treated Mean (±SD)**
Oxygen consumption rate (pmol/min)		
Basal respiration	82.6 ± 0.8	73.7 ± 4.0
Maximal respiration	284.1 ± 16.6	183.2 ± 13.8
Spare respiration capacity	201.5 ± 16.2	109.5 ± 10.5
Extra-cellular acidification rate (mpH/min)		
Glycolysis	12.1 ± 3.0	13.8 ± 2.8
Glycolytic capacity	31.5 ± 4.9	37.6 ± 3.5
Non-glycolytic acidification	6.5 ± 0.8	12.2 ± 2.7
Real-time qRT-PCR (Fold change)		
MFN1	0.74 ± 0.14	0.77 ± 0.04
MFN2	1.10 ± 0.03	1.13 ± 0.15
PGC-1α	2.88 ± 0.20	5.10 ±0.10
PGC-1β	0.26 ± 0.03	0.25 ± 0.01
DRP1	0.37 ± 0.01	0.35 ± 0.16
FIS1	0.92 ± 0.01	0.80 ± 0.09
Mitochondrial membrane potential (Normalized fluorescence intensity)	0.85 ± 0.11	0.60 ± 0.12

Abbreviations: Lipo-doxo: Pegylated Liposomal Doxorubicin HCl; PGC-1α: Peroxisome Proliferator-Activated Receptor Gamma Coactivator-1alpha; PGC-1β: Peroxisome Proliferator-Activated Receptor Gamma Coactivator-1beta; DRP1: Dynamin-Related Protein 1; FIS1: Fission1; MFN1: Mitofusin1; MFN2: Mitofusin2; qRT-PCR: Quantitative Reverse Transcription PCR; SD: Standard Deviation

well-tolerated drug for treating individuals with type 2 diabetes. Metformin inhibits growth of breast cancer cell lines [50,51], blocks cellular transformation in an inducible model system [52,53], and has anti-tumor effects in mouse xenografts [52-55]. Furthermore, in mouse xenografts involving a human breast cancer cell line, co-injection of metformin and doxorubicin intra-peritoneally near the tumor increases the rate of tumor regression compared to treatment with doxorubicin alone, and this combinatorial therapy prevents relapse for at least several months [52]. The results from the present study support the notion that Lipo-doxo is more toxic under high glucose compared to normal glucose conditions (Table 1). This implies that chemotherapy drugs cause damage not only to cancer cells, but also normal cells especially at high doses under high glucose conditions. Our results are in agreement with previous studies which showed that short-term starvation can selectively sensitize cancer cells to chemotherapeutics, while simultaneously protecting normal cells from their side effects via the insulin-like growth factor 1 pathway and the regulation of the glucose levels [9].

CONCLUSION

The present data suggest that treatment of C2C12 myoblast cells with Lipo-doxo down-regulated the expression of MFN1, PGC-1β, FIS1, and DRP1 genes and up-regulated the expression of PGC-1α and MFN2 genes, and likely thereby altered the mitochondrial membrane potential and reduced mitochondrial function. Lipo-doxo treatment also significantly reduced both mitochondrial oxygen consumption rate and extra cellular acidification rate under high glucose and normal glucose conditions in a dose dependent manner. There were several morphological alterations after treatment of C2C12 myoblasts with 30 μg/mL Lipo-doxo for 24 h under high glucose stress conditions including nuclear swelling and the formation of vacuoles. This study may help in the development of new studies on therapeutic targets for preserving mitochondria and preventing myocardial damage associated with the use of Lipo-doxo in treatment of a variety of cancers.

ACKNOWLEDGEMENTS

This study was supported in part by the Claude D. Pepper Older American Independence Center grant (P30AG28718). We thank Laura Gocio for the assistance with the manuscript preparation.

REFERENCES

1. Larsson SC, Mantzoros CS, Wolk A. Diabetes mellitus and risk of breast cancer: A meta-analysis. Int J Cancer. 2007; 121: 856-862.
2. Hsu IR, Kim SP, Kabir M, Bergman RN. Metabolic syndrome, hyperinsulinemia, and cancer. Am J Clin Nutr. 2007; 86: 867-871.
3. Duan W, Shen X, Lei J, Xu Q, Yu Y, Li R, et al. Hyperglycemia, a Neglected Factor during Cancer Progression. BioMed Res Int. 2014; 2014: 10.
4. Brunello A, Kapoor R, Extermann M. Hyperglycemia During Chemotherapy for Hematologic and Solid Tumors Is Correlated With Increased Toxicity. Am J Clin Oncol. 2011; 34: 292-296.
5. Rose PG. Pegylated liposomal doxorubicin: optimizing the dosing schedule in ovarian cancer. Oncologist. 2005; 10: 205-214.
6. Rahman AM, Yusuf SW, Ewer MS. Anthracycline-induced cardiotoxicity and the cardiac-sparing effect of liposomal formulation. Int J Nanomed. 2007; 2: 567-583.
7. Zhang S, Liu X, Bawa-Khalfe T, Lu L-S, Lyu YL, Liu LF, et al. Identification of the molecular basis of doxorubicin-induced cardiotoxicity. Nat Med. 2012; 18: 1639-1642.
8. Carvalho FS, Burgeiro A, Garcia R, Moreno AJ, Carvalho RA, Oliveira PJ. Doxorubicin-induced cardiotoxicity: from bioenergetic failure and cell death to cardiomyopathy. Medl Res Rev. 2014; 34: 106-135.
9. Todorova VK, Makhoul I, Siegel ER, Wei J, Stone A, Carter W, et al. Biomarkers for Presymptomatic Doxorubicin-Induced Cardiotoxicity in Breast Cancer Patients. PLoS ONE. 2016; 11: e0160224.
10. Xu MF, Tang PL, Qian ZM, Ashraf M. Effects by doxorubicin on the myocardium are mediated by oxygen free radicals. Life Sci. 2001; 68: 889-901.
11. Westermann B. Mitochondrial fusion and fission in cell life and death. Nat Rev Mol Cell Biol. 2010; 11: 872-884.
12. Frazier Ann E, Kiu C, Stojanovski D, Hoogenraad Nicholas J, Ryan Michael T. Mitochondrial morphology and distribution in mammalian cells. Biol Chem. 2006; 387: 1551-1558.
13. Song M, Mihara K, Chen Y, Scorrano L, Dorn Ii Gerald W. Mitochondrial fission and fusion factors reciprocally orchestrate mitophagic culling in mouse hearts and cultured fibroblasts. Cell Metab. 2015; 21: 273-285.
14. Dietrich Marcelo O, Liu Z-W, Horvath Tamas L. Mitochondrial dynamics controlled by mitofusins regulate agrp neuronal activity and diet-induced obesity. Cell. 2013; 155: 188-199.
15. Ranieri M, Brajkovic S, Riboldi G, Ronchi D, Rizzo F, Bresolin N, et al. Mitochondrial fusion proteins and human diseases. Neurol Res Int. 2013; 2013: 11.
16. Nunnari J, Suomalainen A. Mitochondria: in sickness and in health. Cell. 2012; 148: 1145-1159.
17. Wu M, Neilson A, Swift AL, Moran R, Tamagnine J, Parslow D, et al. Multiparameter metabolic analysis reveals a close link between attenuated mitochondrial bioenergetic function and enhanced glycolysis dependency in human tumor cells. Am J Physiol Cell Physiol. 2007; 292: C125-C136.
18. Meeusen S, McCaffery JM, Nunnari J. Mitochondrial fusion intermediates revealed *in vitro*. Science. 2004; 305: 1747-1752.
19. Koshiba T, Detmer SA, Kaiser JT, Chen H, McCaffery JM, Chan DC. Structural basis of mitochondrial tethering by mitofusin complexes. Science. 2004; 305: 858-862.
20. Macho A, Decaudin D, Castedo M, Hirsch T, Susin SA, Zamzami N, et al. Chloromethyl-X-rosamine is an aldehyde-fixable potential-sensitive fluorochrome for the detection of early apoptosis. Cytometry. 1996; 25: 333-340.
21. Krysko DV, Roels F, Leybaert L, D'Herde K. Mitochondrial transmembrane potential changes support the concept of mitochondrial heterogeneity during apoptosis. J Histochem Cytochem. 2001; 49: 1277-1284.
22. Weissig V. From Serendipity to Mitochondria-Targeted Nanocarriers. Pharm Res. 2011; 28: 2657.
23. Vaidya B, Paliwal R, Rai S, Khatri K, Goyal AK, Mishra N, et al. Cell-selective mitochondrial targeting: A new approach for cancer therapy. Cancer Ther. 2009; 7: 141-148.
24. Wang X, Shao N, Zhang Q, Cheng Y. Mitochondrial targeting dendrimer allows efficient and safe gene delivery. J Mater Chem B. 2014; 2: 2546-

2553.

25. Battigelli A, Russier J, Venturelli E, Fabbro C, Petronilli V, Bernardi P, et al. Peptide-based carbon nanotubes for mitochondrial targeting. Nanoscale. 2013; 5: 9110-9117.

26. Chang HI, Yeh MK. Clinical development of liposome-based drugs: formulation, characterization, and therapeutic efficacy. Int J Nanomed. 2012; 7: 49-60.

27. Yamada Y, Akita H, Kogure K, Kamiya H, Harashima H. Mitochondrial drug delivery and mitochondrial disease therapy – An approach to liposome-based delivery targeted to mitochondria. Mitochondrion. 2007; 7: 63-71.

28. Green PS, Leeuwenburgh C. Mitochondrial dysfunction is an early indicator of doxorubicin-induced apoptosis. Biochim Biophys Acta (BBA). 2002; 1588: 94-101.

29. Papadopoulou LC, Theophilidis G, Thomopoulos GN, Tsiftsoglou AS. Structural and functional impairment of mitochondria in adriamycin-induced cardiomyopathy in mice: suppression of cytochrome c oxidase II gene expression. Biochem Pharmacol. 1999; 57: 481-489.

30. Goormaghtigh E, Huart P, Praet M, Brasseur R, Ruysschaert JM. Structure of the adriamycin-cardiolipin complex. Biophys Chem. 1990; 35: 247-257.

31. Brand Martin D, Nicholls David G. Assessing mitochondrial dysfunction in cells. Biochem J. 2011; 435: 297-312.

32. Hill BG, Dranka BP, Zou L, Chatham JC, Darley-Usmar VM. Importance of the bioenergetic reserve capacity in response to cardiomyocyte stress induced by 4-hydroxynonenal. Biochem J. 2009; 424: 99-107.

33. Hill BG, Benavides GA, Lancaster JR, Ballinger S, Dell'Italia L, Zhang J, et al. Integration of cellular bioenergetics with mitochondrial quality control and autophagy. Biol Chem. 2012; 393: 1485-1512.

34. Souid AK, Penefsky HS, Sadowitz PD, Toms B. Enhanced cellular respiration in cells exposed to doxorubicin. Mol Pharm. 2006; 3: 307-321.

35. Souid AK, Tacka KA, Galvan KA, Penefsky HS. Immediate effects of anticancer drugs on mitochondrial oxygen consumption. Biochem Pharmacol. 2003; 66: 977-987.

36. Liesa M, Borda-d'Água B, Medina-Gómez G, Lelliott CJ, Paz JC, Rojo M, et al. Mitochondrial fusion is increased by the nuclear coactivator PGC-1β. PLoS ONE. 2008; 3: e3613.

37. Martin OJ, Lai L, Soundarapandian MM, Leone TC, Zorzano A, Keller MP, et al. A role for PGC-1 coactivators in the control of mitochondrial dynamics during postnatal cardiac growth. Circ Res. 2014; 114: 626-636.

38. Papanicolaou KN, Kikuchi R, Ngoh GA, Coughlan KA, Dominguez I, Stanley WC, et al. Mitofusins 1 and 2 are essential for postnatal metabolic remodeling in heart. Circ Res. 2012; 111: 1012-1026.

39. Wallace DC. A Mitochondrial paradigm of metabolic and degenerative diseases, aging, and cancer: a dawn for evolutionary medicine. Annu Rev Genet. 2005; 39: 359.

40. Perry SW, Norman JP, Barbieri J, Brown EB, Gelbard HA. Mitochondrial membrane potential probes and the proton gradient: a practical usage guide. BioTechniques. 2011; 50: 98-115.

41. Eisner V, Lenaers G, Hajnóczky G. Mitochondrial fusion is frequent in skeletal muscle and supports excitation–contraction coupling. J Cell Biol. 2014; 205: 179-195.

42. Sardão VA, Oliveira PJ, Holy J, Oliveira CR, Wallace KB. Morphological alterations induced by doxorubicin on H9c2 myoblasts: nuclear, mitochondrial, and cytoskeletal targets. Cell Biol Toxicol. 2009; 25: 227-243.

43. Dudnakova TV, Lakomkin VL, Tsyplenkova VG, Shekhonin BV, Shirinsky VP, Kapelko VI. Alterations in myocardial cytoskeletal and regulatory protein expression following a single Doxorubicin injection. J Cardiovascular pharmacol. 2003; 41: 788-794.

44. Kim JE, Han BS, Choi WS, Eom DS, Lee EH, Oh TH, et al. Temporospatial sequence of cellular events associated with etoposide-induced neuronal cell death: Role of antiapoptotic protein Bcl-XL. J Neurosci Res. 2001; 66: 1074-1082.

45. Iwasaki T, Suzuki T. Ultrastructural alterations of the myocardium induced by doxorubicin. Virchows Archiv B. 1991; 60: 35-39.

46. Yan L, Vatner DE, Kim SJ, Ge H, Masurekar M, Massover WH, et al. Autophagy in chronically ischemic myocardium. PNAS USA. 2005; 102: 13807-13812.

47. Terman A, Brunk UT. Autophagy in cardiac myocyte homeostasis, aging, and pathology. Cardiovasc Res. 2005; 68: 355-365.

48. Evans JMM, Donnelly LA, Emslie-Smith AM, Alessi DR, Morris AD. Metformin and reduced risk of cancer in diabetic patients. BMJ. 2005; 330: 1304-1305.

49. Jiralerspong S, Palla SL, Giordano SH, Meric-Bernstam F, Liedtke C, Barnett CM, et al. Metformin and Pathologic Complete Responses to Neoadjuvant Chemotherapy in Diabetic Patients With Breast Cancer. J Clin Oncol. 2009; 27: 3297-3302.

50. Alimova IN, Liu B, Fan Z, Edgerton SM, Dillon T, Lind SE, et al. Metformin inhibits breast cancer cell growth, colony formation and induces cell cycle arrest in vitro. Cell Cycle. 2009; 8: 909-915.

51. Liu B, Fan Z, Edgerton SM, Deng XS, Alimova IN, Lind SE, et al. Metformin induces unique biological and molecular responses in triple negative breast cancer cells. Cell Cycle. 2009; 8: 2031-2040.

52. Hirsch HA, Iliopoulos D, Tsichlis PN, Struhl K. Metformin Selectively Targets Cancer Stem Cells, and Acts Together with Chemotherapy to Block Tumor Growth and Prolong Remission. Cancer Res. 2009; 69: 7507-7511.

53. Hirsch HA, Iliopoulos D, Joshi A, Zhang Y, Jaeger SA, Bulyk M, et al. A Transcriptional Signature and Common Gene Networks Link Cancer with Lipid Metabolism and Diverse Human Diseases. Cancer Cell. 2010; 17: 348-361.

54. Anisimov VN, Egormin PA, Piskunova TS, Popovich IG, Tyndyk ML, Yurova MN, et al. Metformin extends life span of HER-2/neu transgenic mice and in combination with melatonin inhibits growth of transplantable tumors in vivo. Cell Cycle. 2010; 9: 188-197.55.

55. Dowling RJO, Zakikhani M, Fantus IG, Pollak M, Sonenberg N. Metformin Inhibits Mammalian Target of Rapamycin–Dependent Translation Initiation in Breast Cancer Cells. Cancer Res. 2007; 67: 10804-10812.

Cite this article

Ameer FS, Zhang X, Azhar G, Wei JY (2018) The Effect of Pegylated Liposomal Doxorubicin HCl on Cellular Mitochondrial Function. J Pharmacol Clin Toxicol 6(1):1099.